Ill-posedness in 2D Mixed Sediment River Morphodynamics

Report

Authors:

Víctor Chavarrías [1]
Willem Ottevanger [2]
Ralph Schielen [3]
Astrid Blom [1]

[1] Faculty of Civil Engineering and Geosciences, Delft University of Technology, Delft, The Netherlands.
[2] Deltares, Delft, The Netherlands.
[3] Rijkswaterstaat, Lelystad, The Netherlands.

Version: 1.1.208 DRAFT compiled on 2017/11/20 AT 12:37

Preface

This document is a concept report (*concept rapportage*) of the project "Ellipticity implementation in D3D" (RWS *bestelnummer* 4500268550, TUD *kenmerk* 17363). We present the overall structure of the final report. The text in red highlights incomplete sections.

Abstract

The currently applied model for predicting mixed-sediment river morphodynamics at large spatial scales and long time scales may be ill-posed under certain circumstances. In these conditions produces unphysical and unrealistic results. The conditions in which the model loses its predictive capabilities have been thoroughly studied under the assumption of one-dimensional flow. In this project we extend the analysis to two-dimensional conditions. We implement a routine in the software package Delft3D to check whether simulations run with this software suffer from ill-posedness.

Contents

1 Introduction

In modeling the morphodynamic change of a river, estuary or the coast, most often a set of equations representing flow is solved in combination with an equation accounting for mass conservation of bed sediment. This approach, however, does not capture the mixed character of the sediment. The mixed character of the sediment in alluvial rivers is a property necessary to explain physical phenomena such as downstream fining (*Sternberg*, 1875; *Blom et al.*, 2016), the gravel sand transition zone (*Yatsu*, 1955), the formation of bedload sheets (*Seminara et al.*, 1996), the evolution of bars (*Lanzoni and Tubino*, 1999), and bed surface armoring (*Parker and Klingeman*, 1982).

The currently applied model for predicting mixed-sediment river morphodynamics at large spatial scales and long time scales is the active layer model (*Hirano*, 1971). This is a deterministic model where the bed is discretized into layers and the sediment mixture in a finite number of size fractions. The topmost layer (the active layer) interacts with the flow (i.e., the sediment transport and friction depend on the conditions of this layer) while the layers below (the substrate) only act as bookkeeping system. There is a sediment flux from and to the active layer if there is a time variation of the elevation of the interface between the active layer and the substrate.

This model has proven its value over a wide range of different situations for decades. Nevertheless under some circumstances the model may be ill-posed (*Ribberink*, 1987; *Stecca et al.*, 2014; *Chavarrías et al.*) and in these conditions produces unphysical and unrealistic results (*Joseph and Saut*, 1990; *Chavarrías et al.*).

There are alternatives to the active layer model such as the one by *Ribberink* (1987) where a second active layer is taken into account. This model was derived for dune-dominated cases and it does not solve the problem of ill-posedness (*Sieben*, 1997). The continuous model by *Blom et al.* (2003, 2006, 2008) was also derived for dune dominated cases and it is not applicable at large space scales or long time scales (*Blom*, 2008). A simplified continuous model derived by *Viparelli et al.* (2017) is applicable at large scale but it can also become ill-posed (*Chavarrías et al.*). Thus, the active layer model is still the main model for predicting mixed sediment river morphodynamics.

When the relevant morphodynamic characteristics can be well reproduced in a one-dimensional approach, the flow is often represented by the *Saint-Venant* (1871) equations. The conditions under which this system of equations can be ill-posed have been studied by, for instance, *Ribberink* (1987), *Sieben* (1997), and *Stecca et al.* (2014). When flow curvature plays a significant role in the morphodynamics the one-dimensional approach is no longer valid. This fact is clearly seen in river bends where the curvature of the flow creates a shallower inner bend and deeper outer bend as was first observed and explained by *Thomson* (1876). In these cases the flow is intrinsically three-dimensional and is characterized by a mean flow and a secondary or spiral flow. For large temporal and spatial scales as typically occurs in engineering applications, it is not feasible to solve a three-dimensional system of equations. However, the secondary flow can be parametrized and included in a two-dimensional system of equations (i.e., the Shallow Water Equations), considerably reducing the computational time (*Kalkwijk and Booij*, 1986). The parametrization is based on the intensity of the secondary flow I which is a measure of the magnitude of the velocity component normal to the depth-averaged velocity. An advection-diffusion equation models this variable which is found in extra terms in the momentum equations. Thus, the consideration of secondary flow not only modifies the momentum equations but also adds an extra equation to the system. *Chavarrías and Ottevanger* (2016) studied the mathematical character of the system of equations formed by the Shallow Water Equations in combination with the active layer model. However, they did not study the effect of considering secondary flow. They implemented a routine in the software package Delft3D to obtain the parameters needed to assess the well-posedness of a simulation. Yet, the actual check on the parameters was not implemented. Moreover, they did not study the implications of ill-posedness in 2D numerical simulations.

The objective of this project is to extend the previous analysis by including secondary flow. An analytical study of the system of equations will shed light on the relative importance of this specific mechanism with emphasis on the role of diffusive processes on the mathematical character of the system of equations. We aim at showing the consequences of ill-posedness in 2D numerical simulations and to assess the implications for field cases.

The report is organized as follows. In Section 2 we summarize the research questions. The model equations are shown in Section 3. In Section 4 we linearize the system of equations. In Section 5 we present the results of the linear analysis. In Section 6 we discuss the implementation of the check in Delft3D together with the results of its application to numerical simulations. In Section 7 we discuss our results and sketch the future work. In Section 8 we present the main conclusions.

2 Research Questions and Methodology

Our objective is to study the mathematical character of the system of equations used to model mixed-sediment morphodynamics in two dimensions. We will focus on the following research questions:

1. What is the role of secondary flow as regards to the mathematical character of the system of equations?
2. What are the consequences of ill-posedness in 2D numerical simulations?
3. What are the implications of ill-posedness in field cases?

To answer Research Question 1 we will conduct a mathematical analysis of the system of equations composed by the Shallow Water Equations in combination with the active layer model and secondary flow. We will assess the role of diffusive processes as well as the relative importance of the different physical mechanism.

To answer Research Question 2 we will finish the implementation of the check tool in Delft3D. Then, the tool will be extended accounting for secondary flow. Once the tool is validated, it will be applied to idealized simulations to get insight on the consequences of ill-posedness.

To answer Research Question 3 we will run simulations which, rather than idealized, resemble the conditions frequently found in field cases.

Eventually, we will write a report presenting the results.

3 Model Equations

In this section we describe the equations that model shallow water flow with a parametrized secondary flow correction together with the active layer model of *Hirano* (1971). These equations represent hydrostatic flow over a mobile bed composed of several (N) non-cohesive sediment fractions. In Section 3.1 we write the model equations. In Section 3.2 we simplify the equations. In Section 3.3 we describe the closure relations of the model. The equations are expanded in Section 3.4 to write them in matrix form (Section 3.5).

3.1 Balance Equations

The equations we use are:

- Water mass conservation:
$$\frac{\partial h}{\partial t} + \frac{\partial q_x}{\partial x} + \frac{\partial q_y}{\partial y} = 0 \tag{1}$$
- Water momentum conservation in x direction:
$$\frac{\partial q_x}{\partial t} + \frac{\partial (q_x^2/h + gh^2/2)}{\partial x} + \frac{\partial \left(\frac{q_x q_y}{h}\right)}{\partial y} + gh\frac{\partial \eta}{\partial x} - F'_{sx} = -ghS_{fx} \tag{2}$$
- Water momentum conservation in y direction:
$$\frac{\partial q_y}{\partial t} + \frac{\partial (q_y^2/h + gh^2/2)}{\partial y} + \frac{\partial \left(\frac{q_x q_y}{h}\right)}{\partial x} + gh\frac{\partial \eta}{\partial y} - F'_{sy} = -ghS_{fy} \tag{3}$$
- Constitutive equation for the secondary flow intensity:
$$\frac{\partial I}{\partial t} + \frac{q_x}{h}\frac{\partial I}{\partial x} + \frac{q_y}{h}\frac{\partial I}{\partial y} - D_H\frac{\partial^2 I}{\partial x^2} - D_H\frac{\partial^2 I}{\partial y^2} = S_s \tag{4}$$
- Sediment mass conservation for the entire mixture (Exner):
$$\frac{\partial \eta}{\partial t} + \frac{\partial q_{bx}}{\partial x} + \frac{\partial q_{by}}{\partial y} = 0 \tag{5}$$
- Sediment mass conservation per grain size in the active layer (Hirano):
$$\frac{\partial M_{ak}}{\partial t} + f_k^I\frac{\partial (\eta - L_a)}{\partial t} + \frac{\partial q_{bkx}}{\partial x} + \frac{\partial q_{bky}}{\partial y} = 0 \quad k \in \{1, N-1\} \tag{6}$$
- Sediment mass conservation per grain size in the substrate:
$$\frac{\partial M_{sk}}{\partial t} - f_k^I\frac{\partial (\eta - L_a)}{\partial t} = 0 \quad k \in \{1, N-1\} \tag{7}$$

where:

- x = Cartesian x coordinate $[m]$
- y = Cartesian y coordinate $[m]$
- t = time coordinate $[s]$
- h = flow depth $[m]$
- q_x = specific water discharge in x direction $[m^2/s]$
- q_y = specific water discharge in y direction $[m^2/s]$
- η = bed elevation $[m]$
- f_k^I = volume fraction content of size fraction k at the interface between the active layer and the substrate $[-]$
- L_a = active layer thickness $[m]$
- q_{bkx} = sediment transport of size fraction k (including pores) in x direction $[m^2/s]$
- q_{bky} = sediment transport of size fraction k (including pores) in y direction $[m^2/s]$
- q_{bx} = total sediment transport (including pores) in x direction $[m^2/s]$
- q_{by} = total sediment transport (including pores) in y direction $[m^2/s]$
- S_{fx} = friction slope in the x direction $[-]$
- S_{fy} = friction slope in the y direction $[-]$
- g = acceleration due to gravity $[m/s^2]$
- $M_{ak} = F_{ak} L_a$ = volume of sediment of size fraction k in the active layer per unit of surface area $[m]$
- F_{ak} = volume fraction content of size fraction k in the active layer $[-]$
- $M_{sk} = \int_{\eta_0}^{\eta - L_a} f_{sk}(z)\mathrm{d}z$ = volume of sediment of size fraction k in the substrate per unit of surface area $[m]$
- η_0 = reference bed elevation $[m]$
- f_{sk} = volume fraction of size fraction k in the substrate $[-]$
- N = number of size fractions $[-]$
- F'_{sx} = force per unit mass along the flow depth due to the secondary flow in the x direction $[m^2/s^2]$
- F'_{sy} = force per unit mass along the flow depth due to the secondary flow in the y direction $[m^2/s^2]$
- I = secondary flow intensity $[m/s]$
- D_H = horizontal diffusion coefficient $[m^2/s]$
- S_s = source term due to secondary flow $[m/s]$

The volume fraction content of sediment at the active layer and the substrate are constrained by the equations:

$$\sum_{k=1}^{N} F_{ak} = 1, \quad \sum_{k=1}^{N} f_{sk}(z) = 1 \ , \tag{8}$$

thus, the volume of sediment per unit area are constrained by the equations:

$$\sum_{k=1}^{N} M_{ak} = L_a, \quad \sum_{k=1}^{N} M_{sk} = \eta - L_a - \eta_0 \ . \tag{9}$$

3.2 Simplifications

We:

1. assume a constant active layer thickness:

$$\frac{\partial L_a}{\partial t} = 0 \tag{10}$$

Substitution of Equation 10 in 6 and 7 yields:

$$\frac{\partial M_{ak}}{\partial t} - f_k^I \frac{\partial q_{bx}}{\partial x} - f_k^I \frac{\partial q_{by}}{\partial y} + \frac{\partial q_{bkx}}{\partial x} + \frac{\partial q_{bky}}{\partial y} = 0 \quad k \in \{1, N-1\} \tag{11}$$

$$\frac{\partial M_{sk}}{\partial t} + f_k^I \frac{\partial q_{bx}}{\partial x} + f_k^I \frac{\partial q_{by}}{\partial y} = 0 \quad k \in \{1, N-1\} \tag{12}$$

3.3 Closure Relations

The governing equations still need closure relations for the friction slope, the sediment transport rate, the secondary flow terms, and the fractions at the interface between the substrate and the active layer to form a complete set of equations. In this section we describe those closure relations.

3.3.1 Friction Slope

The friction slope is:

$$S_{fx} = \frac{C_f q_x Q}{g h^3} \quad S_{fy} = \frac{C_f q_y Q}{g h^3} \tag{13}$$

where:

- C_f = dimensionless friction coefficient $[-]$
- $Q = |\vec{q}|$ = module of the specific water discharge $[m/s^2]$

3.3.2 Sediment Transport Rate

The sediment transport rate per size fraction (including pores) $\vec{q_{bk}}$ $[m^2/s]$ can be expressed as:

$$\vec{q_{bk}} = (q_{bkx}, q_{bky}) = q_{bk}(\cos\varphi_{sk}, \sin\varphi_{sk}) \quad k \in \{1, N\} \tag{14}$$

where:

- φ_{sk} = direction of the sediment transport rate (correcting for bed slope and secondary flow) [rad]
- q_{bk} = absolute value of the sediment transport rate including pores $[m^2/s]$

The direction of the sediment transport rate φ_{sk} [rad] is:

$$\tan\varphi_{sk} = \frac{\sin\varphi_\tau - \frac{1}{g_{sk}}\frac{\partial \eta}{\partial y}}{\cos\varphi_\tau - \frac{1}{g_{sk}}\frac{\partial \eta}{\partial x}} \quad k \in \{1, N\} \tag{15}$$

where:

- φ_τ = direction of the sediment transport rate only correcting for secondary flow $[rad]$
- g_{sk} = bed slope function $[-]$

The direction of the sediment transport rate φ_τ [rad] is:

$$\tan\varphi_\tau = \frac{q_y - h\alpha_I \frac{q_x}{Q} I}{q_x - h\alpha_I \frac{q_y}{Q} I} \tag{16}$$

where:

- α_I = constant $[-]$

The constant α_I [−] is:

$$\alpha_I = \frac{2}{\kappa^2} E_s \left(1 - \frac{\sqrt{C_f}}{2\kappa}\right) \tag{17}$$

where:

- κ = Von Kármán constant [−]
- E_s = calibration parameter [−]

The bed slope function g_{sk} is:

$$g_{sk} = A_s \theta_k^{B_s} \left(\frac{d_k}{h}\right)^{C_s} \left(\frac{d_k}{D_m}\right)^{D_s} \tag{18}$$

where:

- A_s = calibration constant [−]
- B_s = calibration constant [−]
- C_s = calibration constant [−]
- D_s = calibration constant [−]
- θ_k = module of the Shields stress of size fraction k [−]
- d_k = characteristic grain size of size fraction k $[m]$
- D_m = characteristic mean grain size of the mixture $[m]$

Values for the constants are summarized in Table 1.

A_s	B_s	C_s	D_s	Note
1.70	0.5	0.0	0.0	*Talmon et al.* (1995) (their experiments, straigh flume)
0.85	0.5	0.0	0.0	*Talmon et al.* (1995) (experiments by *Zimmerman and Kennedy* (1978), circular flume)
9.00	0.5	0.3	0.0	*Talmon et al.* (1995) (2D runs of field and lab)

Table 1: Parameters of the function for the bed slope.

The absolute value of the sediment transport rate is:

$$q_{bk} = F_{ak} \sqrt{g R d_k^3} \, (1-p) \, q_{bk}^* \quad k \in \{1, N\} \, , \tag{19}$$

where:

- q_{bk}^* = nondimensional sediment transport rate [−]
- p = porosity [−]
- $R = \rho_s/\rho_w - 1$ = submerged sediment density [−]
- $\rho_s = 2650$ = sediment density $[kg/m^3]$
- $\rho_w = 1000$ = water density $[kg/m^3]$

The nondimensional sediment transport rate is computed using, for instance, a generalized form of the relation developed by *Meyer-Peter and Müller* (1948)

$$q_{bk}^* = A \max\left(\theta_k - \xi_k \theta_c, 0\right)^B \quad k \in \{1, N\} \, , \tag{20}$$

where:

- A = nondimensional parameter [−]
- B = nondimensional parameter [−]
- θ_c = nondimensional critical bed shear stress [−]

- ξ_k = hiding coefficient $[-]$

The module of the Shields stress is:

$$\theta_k = \frac{C_f \left(\frac{Q}{h}\right)^2}{gRd_k} \quad k \in \{1, N\} \tag{21}$$

A common hiding functions is the one due to *Egiazaroff* (1965):

$$\xi_k = \left(\frac{\log_{10}(19)}{\log_{10}\left(19\frac{d_k}{D_m}\right)}\right)^2 \quad k \in \{1, N\} \tag{22}$$

A simpler expression was developed by *Parker et al.* (1982):

$$\xi_k = \left(\frac{D_m}{d_k}\right)^b \quad k \in \{1, N\} \tag{23}$$

where:

- b = nondimensional parameter $[-]$

3.3.3 Secondary Flow Terms

The secondary flow terms in the momentum equations are:

$$F'_{sx} = \frac{\partial T'_{xx}}{\partial x} + \frac{\partial T'_{xy}}{\partial y} \tag{24}$$

$$F'_{sy} = \frac{\partial T'_{yx}}{\partial x} + \frac{\partial T'_{yy}}{\partial y} \tag{25}$$

where:

- T'_{lm} = shear stress per unit mass and volume along the flow depth in the direction l-m $[m^3/s^2]$

The closure relation for the secondary flow force terms are:

$$T'_{xx} = -2\frac{\beta^* I}{Q} q_x q_y \tag{26}$$

$$T'_{xy} = T'_{yx} = \frac{\beta^* I}{Q}\left(q_x^2 - q_y^2\right) \tag{27}$$

$$T'_{yy} = T'_{yy} = 2\frac{\beta^* I}{Q} q_x q_y \tag{28}$$

where:

- $\beta^* = \beta_c\left(5\alpha - 15.6\alpha^2 + 37.5\alpha^3\right)$ = constant $[-]$
- $\beta_c \in [0, 1]$ = calibration parameter $[-]$
- $\alpha = \frac{\sqrt{C_f}}{\kappa} < 0.5$ = constant $[-]$

The closure relation for the source term of the secondary flow equation (4) is:

$$Ss = -\frac{I - I_e}{T_I} \tag{29}$$

where:

- $I_e = Q/R_s$ = equilibrium secondary flow intensity $[m/s]$
- T_I = adaptation time scale $[s]$
- R_s = radius of curvature of the streamlines $[m]$

The radius of curvature of the streamlines is defined as:

$$\frac{1}{R_s} = \frac{\frac{\mathrm{d}x}{\mathrm{d}t}\frac{\mathrm{d}^2y}{\mathrm{d}t^2} - \frac{\mathrm{d}y}{\mathrm{d}t}\frac{\mathrm{d}^2x}{\mathrm{d}t^2}}{\left(\left(\frac{\mathrm{d}x}{\mathrm{d}t}\right)^2 + \left(\frac{\mathrm{d}y}{\mathrm{d}t}\right)^2\right)^{3/2}} , \tag{30}$$

substituting $u = \frac{\mathrm{d}x}{\mathrm{d}t}$ and $v = \frac{\mathrm{d}y}{\mathrm{d}t}$ we obtain:

$$\frac{1}{R_s} = \frac{u\frac{\mathrm{d}v}{\mathrm{d}t} - v\frac{\mathrm{d}u}{\mathrm{d}t}}{\left(u^2+v^2\right)^{3/2}} , \tag{31}$$

expanding the material derivatives and assuming steady flow we obtain:

$$\frac{1}{R_s} = \frac{u^2\frac{\partial v}{\partial x} + uv\frac{\partial v}{\partial y} - uv\frac{\partial u}{\partial x} - v^2\frac{\partial u}{\partial y}}{\left(u^2+v^2\right)^{3/2}} , \tag{32}$$

in terms of water discharge we obtain:

$$\frac{1}{R_s} = \frac{-q_xq_y\frac{\partial q_x}{\partial x} + q_x^2\frac{\partial q_y}{\partial x} - q_y^2\frac{\partial q_x}{\partial y} + q_xq_y\frac{\partial q_y}{\partial y}}{\left(q_x^2+q_y^2\right)^{3/2}} . \tag{33}$$

The adaptation time scale T_I is:

$$T_I = \frac{L_I h}{Q} \tag{34}$$

where:

- $L_I = L_I^* h$ = adaptation length scale $[m]$
- $L_I^* = \frac{1-2\alpha}{2\kappa^2\alpha}$ = nondimensional adaptation length scale $[-]$

3.3.4 Volume Fraction Content at the Interface

The volume fraction content at the interface between the active layer and the substrate under degradational conditions is assumed to be equal to the volume fraction content at the top part of the substrate. Under aggradational conditions *Hirano* (1971) proposed the flux to the substrate to have the same grain size distribution as the active layer. *Parker* (1991) introduced the concept that the aggradational flux to the substrate is also influenced by the grain size distribution of the bed load. *Hoey and Ferguson* (1994) combined both concepts in a parameter that sets the contribution of the bed load relative to the active layer. Currently, only the initial concept of Hirano is implemented in Delft3D which in mathematical terms can be written as:

$$f_k^I = \begin{cases} f_{sk}(z = \eta - L_a) & \text{if} \quad \frac{\partial(\eta - L_a)}{\partial t} < 0 \\ F_{ak} & \text{if} \quad \frac{\partial(\eta - L_a)}{\partial t} > 0 \end{cases} \tag{35}$$

3.4 Expansion of the System Equations

All the terms in the model equations need to be expressed as a function of the second derivative, first derivative, linear relation, or source of the dependent variables of the system (i.e., $h, q_x, q_y, I, \eta, M_{ak} \forall k \in \{1, N-1\}$). The terms that need to be decomposed are the secondary flow terms in the momentum equations (Section 3.4.1), the sediment transport rate (Section 3.4.2), and the source term in the constitutive equation for secondary flow (Section 3.4.3). The system equations are written in expanded form in Sections 3.4.4-3.4.9.

3.4.1 Expansion of the Secondary Flow Terms in the Momentum Equations

The secondary flow terms in the momentum equations, Equations (26), (27), and (27) are a function of the specific water discharge and secondary flow intensity only:

$$\begin{aligned} T'_{ij} &= f(q_x, q_y, I) \Rightarrow \\ \Rightarrow \frac{\partial T'_{ij}}{\partial x} &= \frac{\partial T'_{ij}}{\partial q_x}\frac{\partial q_x}{\partial x} + \frac{\partial T'_{ij}}{\partial q_y}\frac{\partial q_y}{\partial x} + \frac{\partial T'_{ij}}{\partial I}\frac{\partial I}{\partial x} \end{aligned} \tag{36}$$

and

$$\Rightarrow \frac{\partial T'_{ij}}{\partial y} = \frac{\partial T'_{ij}}{\partial q_x}\frac{\partial q_x}{\partial y} + \frac{\partial T'_{ij}}{\partial q_y}\frac{\partial q_y}{\partial y} + \frac{\partial T'_{ij}}{\partial I}\frac{\partial I}{\partial y}$$

where $i = (x, y)$ and $j = (x, y)$.

3.4.2 Expansion of the Sediment Transport Rate

The directional sediment transport rates q_{bkx} and q_{bky} are not only a function of the flow velocity in their respective directions but also of the flow velocity in the other direction and the secondary flow intensity:

$$\begin{aligned} q_{bkx} &= f(h, q_x, q_y, I, M_{ak}, \frac{\partial \eta}{\partial x}, \frac{\partial \eta}{\partial y}) \Rightarrow \\ \Rightarrow \frac{\partial q_{bkx}}{\partial x} &= \frac{\partial q_{bkx}}{\partial h}\frac{\partial h}{\partial x} + \frac{\partial q_{bkx}}{\partial q_x}\frac{\partial q_x}{\partial x} + \frac{\partial q_{bkx}}{\partial q_y}\frac{\partial q_y}{\partial x} + \frac{\partial q_{bkx}}{\partial I}\frac{\partial I}{\partial x} \\ &+ \sum_{l=1}^{N-1} \frac{\partial q_{bkx}}{\partial M_{al}}\frac{\partial M_{al}}{\partial x} + \frac{\partial q_{bkx}}{\partial \frac{\partial \eta}{\partial x}}\frac{\partial^2 \eta}{\partial x^2} + \frac{\partial q_{bkx}}{\partial \frac{\partial \eta}{\partial y}}\frac{\partial^2 \eta}{\partial x \partial y} \quad k \in \{1, N\} \end{aligned} \tag{37}$$

and,

$$\begin{aligned} q_{bky} &= f(h, q_x, q_v, I, M_{ak}, \frac{\partial \eta}{\partial x}, \frac{\partial \eta}{\partial y}) \Rightarrow \\ \Rightarrow \frac{\partial q_{bky}}{\partial y} &= \frac{\partial q_{bky}}{\partial h}\frac{\partial h}{\partial y} + \frac{\partial q_{bky}}{\partial q_x}\frac{\partial q_x}{\partial y} + \frac{\partial q_{bky}}{\partial q_y}\frac{\partial q_y}{\partial y} + \frac{\partial q_{bky}}{\partial I}\frac{\partial I}{\partial y} \\ &+ \sum_{l=1}^{N-1} \frac{\partial q_{bky}}{\partial M_{al}}\frac{\partial M_{al}}{\partial y} + \frac{\partial q_{bky}}{\partial \frac{\partial \eta}{\partial x}}\frac{\partial^2 \eta}{\partial x \partial y} + \frac{\partial q_{bky}}{\partial \frac{\partial \eta}{\partial y}}\frac{\partial^2 \eta}{\partial y^2} \quad k \in \{1, N\} \end{aligned} \tag{38}$$

The same holds for the total bed load in x and y direction (q_{bx} and q_{by}). Note that M_{aN} is not an independent variable.

3.4.3 Expansion of the Source Term in the Constitutive Equation for the Secondary Flow

Here we expand the term S_s of Equation (4).

$$S_s = -\frac{I - I_e}{T_I} = \frac{-I}{T_I} + \frac{I_e}{T_I} = \frac{-QI}{h^2 L_I^*} + S_{sxx}\frac{\partial q_x}{\partial x} + S_{syx}\frac{\partial q_y}{\partial x} + S_{sxy}\frac{\partial q_x}{\partial y} + S_{syy}\frac{\partial q_y}{\partial y} \tag{39}$$

where:

$$\begin{aligned} S_{sxx} &= \frac{1}{Qh^2 L_I^*}(-q_x q_y) \\ S_{syx} &= \frac{1}{Qh^2 L_I^*}(q_x^2) \\ S_{sxy} &= \frac{1}{Qh^2 L_I^*}(-q_y^2) \\ S_{syy} &= \frac{1}{Qh^2 L_I^*}(q_x q_y) \end{aligned} \tag{40}$$

3.4.4 Water Mass Conservation

All the terms of Equation (1) are already expanded:

$$\frac{\partial h}{\partial t} + \frac{\partial q_x}{\partial x} + \frac{\partial q_y}{\partial y} = 0 \tag{41}$$

3.4.5 Water Momentum Conservation in x Direction

$$\begin{aligned} &\frac{\partial q_x}{\partial t} + \frac{\partial (q_x^2/h + gh^2/2)}{\partial x} + \frac{\partial \left(\frac{q_x q_y}{h}\right)}{\partial y} + gh\frac{\partial \eta}{\partial x} - F'_{sx} = -ghS_{fx} \implies \\ &\frac{\partial q_x}{\partial t} + \left(gh - \left(\frac{q_x}{h}\right)^2\right)\frac{\partial h}{\partial x} + \left(2\frac{q_x}{h} - \frac{\partial T'_{xx}}{\partial q_x}\right)\frac{\partial q_x}{\partial x} - \frac{\partial T'_{xx}}{\partial q_y}\frac{\partial q_y}{\partial x} - \frac{\partial T'_{xx}}{\partial I}\frac{\partial I}{\partial x} + gh\frac{\partial \eta}{\partial x} + \\ &+ \frac{-q_x q_y}{h^2}\frac{\partial h}{\partial y} + \left(\frac{q_y}{h} - \frac{\partial T'_{xy}}{\partial q_x}\right)\frac{\partial q_x}{\partial x} - \left(\frac{q_x}{h} - \frac{\partial T'_{xy}}{\partial q_y}\right)\frac{\partial q_y}{\partial y} - \frac{\partial T'_{xy}}{\partial I}\frac{\partial I}{\partial y} + \\ &+ \frac{C_f q_x Q}{h^2} = 0 \end{aligned} \tag{42}$$

3.4.6 Water Momentum Conservation in y Direction

$$\begin{aligned}\frac{\partial q_y}{\partial t}+\frac{\partial(q_y^2/h+gh^2/2)}{\partial y}+\frac{\partial\left(\frac{q_xq_y}{h}\right)}{\partial x}+gh\frac{\partial\eta}{\partial y}-F'_{sy}=-ghS_{fy}\implies\\ \frac{\partial q_y}{\partial t}+\frac{-q_xq_y}{h^2}\frac{\partial h}{\partial x}+\left(\frac{q_y}{h}-\frac{\partial T'_{yx}}{\partial q_x}\right)\frac{\partial q_x}{\partial x}+\left(\frac{q_x}{h}-\frac{\partial T'_{yx}}{\partial q_y}\right)\frac{\partial q_y}{\partial x}-\frac{\partial T'_{yx}}{\partial I}\frac{\partial I}{\partial x}+\\ +\left(gh-\left(\frac{q_y}{h}\right)^2\right)\frac{\partial h}{\partial y}-\frac{\partial T'_{yy}}{\partial q_x}\frac{\partial q_x}{\partial y}+\left(2\frac{q_y}{h}-\frac{\partial T'_{yy}}{\partial q_y}\right)\frac{\partial q_y}{\partial y}-\frac{\partial T'_{yy}}{\partial I}\frac{\partial I}{\partial y}+gh\frac{\partial\eta}{\partial y}+\\ +\frac{C_fq_yQ}{h^2}=0\end{aligned}\tag{43}$$

3.4.7 Constitutive Equation for the Secondary Flow

$$\begin{aligned}\frac{\partial I}{\partial t}+\frac{q_x}{h}\frac{\partial I}{\partial x}+\frac{q_y}{h}\frac{\partial I}{\partial y}-D_H\frac{\partial^2 I}{\partial x^2}-D_H\frac{\partial^2 I}{\partial y^2}=S_s\implies\\ \frac{\partial I}{\partial t}-D_H\frac{\partial^2 I}{\partial x^2}-D_H\frac{\partial^2 I}{\partial y^2}-S_{sxx}\frac{\partial q_x}{\partial x}-S_{syx}\frac{\partial q_y}{\partial x}+\frac{q_x}{h}\frac{\partial I}{\partial x}-S_{sxy}\frac{\partial q_x}{\partial y}-S_{syy}\frac{\partial q_y}{\partial y}+\frac{q_y}{h}\frac{\partial I}{\partial y}+\frac{QI}{h^2L_I^*}=0\end{aligned}\tag{44}$$

3.4.8 Sediment Mass Conservation for the Entire Mixture

$$\begin{aligned}\frac{\partial\eta}{\partial t}+\frac{\partial q_{bx}}{\partial x}+\frac{\partial q_{by}}{\partial y}=0\implies\\ \frac{\partial\eta}{\partial t}+\frac{\partial q_{bx}}{\partial h}\frac{\partial h}{\partial x}+\frac{\partial q_{bx}}{\partial q_x}\frac{\partial q_x}{\partial x}+\frac{\partial q_{bx}}{\partial q_y}\frac{\partial q_y}{\partial x}+\frac{\partial q_{bx}}{\partial I}\frac{\partial I}{\partial x}+\sum_{l=1}^{N-1}\frac{\partial q_{bx}}{\partial M_{al}}\frac{\partial M_{al}}{\partial x}+\\ +\frac{\partial q_{by}}{\partial h}\frac{\partial h}{\partial y}\frac{\partial q_{by}}{\partial q_x}\frac{\partial q_x}{\partial y}+\frac{\partial q_{by}}{\partial q_y}\frac{\partial q_y}{\partial y}+\frac{\partial q_{by}}{\partial I}\frac{\partial I}{\partial y}+\sum_{l=1}^{N-1}\frac{\partial q_{by}}{\partial M_{al}}\frac{\partial M_{al}}{\partial y}\end{aligned}\tag{45}$$

3.4.9 Sediment Mass Conservation per Grain Size in the Active Layer

$$\begin{aligned}\frac{\partial M_{ak}}{\partial t}-f_k^I\frac{\partial q_{bx}}{\partial x}-f_k^I\frac{\partial q_{by}}{\partial y}+\frac{\partial q_{bkx}}{\partial x}+\frac{\partial q_{bky}}{\partial y}=0\quad k\in\{1,N-1\}\implies\\ \frac{\partial M_{ak}}{\partial t}+\left[\frac{\partial q_{bkx}}{\partial h}-f_k^I\frac{\partial q_{bx}}{\partial h}\right]\frac{\partial h}{\partial x}+\left[\frac{\partial q_{bkx}}{\partial q_x}-f_k^I\frac{\partial q_{bx}}{\partial q_x}\right]\frac{\partial q_x}{\partial x}+\left[\frac{\partial q_{bkx}}{\partial q_y}-f_k^I\frac{\partial q_{bx}}{\partial q_y}\right]\frac{\partial q_y}{\partial x}+\\ +\left[\frac{\partial q_{bkx}}{\partial I}-f_k^I\frac{\partial q_{bx}}{\partial I}\right]\frac{\partial I}{\partial x}+\sum_{l=1}^{N-1}\left[\frac{\partial q_{bkx}}{\partial M_{al}}-f_k^I\frac{\partial q_{bx}}{\partial M_{al}}\right]\frac{\partial M_{al}}{\partial x}+\\ \left[\frac{\partial q_{bkx}}{\partial h}-f_k^I\frac{\partial q_{bx}}{\partial h}\right]\frac{\partial h}{\partial y}+\left[\frac{\partial q_{bkx}}{\partial q_x}-f_k^I\frac{\partial q_{bx}}{\partial q_x}\right]\frac{\partial q_x}{\partial y}+\left[\frac{\partial q_{bkx}}{\partial q_y}-f_k^I\frac{\partial q_{bx}}{\partial q_y}\right]\frac{\partial q_y}{\partial y}+\\ +\left[\frac{\partial q_{bkx}}{\partial I}-f_k^I\frac{\partial q_{bx}}{\partial I}\right]\frac{\partial I}{\partial y}+\sum_{l=1}^{N-1}\left[\frac{\partial q_{bkx}}{\partial M_{al}}-f_k^I\frac{\partial q_{bx}}{\partial M_{al}}\right]\frac{\partial M_{al}}{\partial y}+\end{aligned}\tag{46}$$

3.5 Matrix Formulation

In this section we write the system of equations in matrix formulation. Equation (12) is a linear combination of equations (11) and (5). The rest of the equations do not depend on M_{sk}. Thus, the substrate equations provide a zero eigenvalue with multiplicity $N-1$. To simplify the writing we omit the substrate equations.

We recast the model Equations, (41), (42), (43), (44), (45), and (46) in matrix form:

$$\frac{\partial\mathbf{Q}}{\partial t}+\mathbf{D_x}\frac{\partial^2\mathbf{Q}}{\partial x^2}+\mathbf{D_y}\frac{\partial^2\mathbf{Q}}{\partial y^2}+\mathbf{C}\frac{\partial^2\mathbf{Q}}{\partial x\partial y}+\mathbf{A_x}\frac{\partial\mathbf{Q}}{\partial x}+\mathbf{A_y}\frac{\partial\mathbf{Q}}{\partial y}+\mathbf{S}=0\tag{47}$$

The dependent variables are h, q_x, q_y, I, η, and M_{ak} for $1\le k\le N-1$:

$$\mathbf{Q}=\begin{bmatrix}h\\q_x\\q_y\\I\\\eta\\\hdashline[M_{ak}]\end{bmatrix}\tag{48}$$

The diffusive matrix in x direction is:

$$\mathbf{D_x} = \left[\begin{array}{ccccc:c} 0 & 0 & 0 & 0 & 0 & [\mathbb{0}] \\ 0 & 0 & 0 & 0 & 0 & [\mathbb{0}] \\ 0 & 0 & 0 & 0 & 0 & [\mathbb{0}] \\ 0 & 0 & 0 & D_H & 0 & [\mathbb{0}] \\ 0 & 0 & 0 & 0 & \frac{\partial q_{bx}}{\partial \frac{\partial \eta}{\partial x}} & [\mathbb{0}] \\ \hdashline [\mathbb{0}] & [\mathbb{0}] & [\mathbb{0}] & [\mathbb{0}] & \left[\frac{\partial q_{bkx}}{\partial \frac{\partial \eta}{\partial x}} - f_k^I \frac{\partial q_{bx}}{\partial \frac{\partial \eta}{\partial x}}\right] & [\mathbb{0}] \end{array}\right] \tag{49}$$

The diffusive matrix in y direction is:

$$\mathbf{D_y} = \left[\begin{array}{ccccc:c} 0 & 0 & 0 & 0 & 0 & [\mathbb{0}] \\ 0 & 0 & 0 & 0 & 0 & [\mathbb{0}] \\ 0 & 0 & 0 & 0 & 0 & [\mathbb{0}] \\ 0 & 0 & 0 & D_H & 0 & [\mathbb{0}] \\ 0 & 0 & 0 & 0 & \frac{\partial q_{by}}{\partial \frac{\partial \eta}{\partial y}} & [\mathbb{0}] \\ \hdashline [\mathbb{0}] & [\mathbb{0}] & [\mathbb{0}] & [\mathbb{0}] & \left[\frac{\partial q_{bky}}{\partial \frac{\partial \eta}{\partial y}} - f_k^I \frac{\partial q_{by}}{\partial \frac{\partial \eta}{\partial y}}\right] & [\mathbb{0}] \end{array}\right] \tag{50}$$

The matrix of cross derivatives is:

$$\mathbf{C} = \left[\begin{array}{ccccc:c} 0 & 0 & 0 & 0 & 0 & [\mathbb{0}] \\ 0 & 0 & 0 & 0 & 0 & [\mathbb{0}] \\ 0 & 0 & 0 & 0 & 0 & [\mathbb{0}] \\ 0 & 0 & 0 & 0 & 0 & [\mathbb{0}] \\ 0 & 0 & 0 & 0 & \frac{\partial q_{bx}}{\partial \frac{\partial \eta}{\partial y}} + \frac{\partial q_{by}}{\partial \frac{\partial \eta}{\partial x}} & [\mathbb{0}] \\ \hdashline [\mathbb{0}] & [\mathbb{0}] & [\mathbb{0}] & [\mathbb{0}] & \left[\frac{\partial q_{bkx}}{\partial \frac{\partial \eta}{\partial y}} - f_k^I \frac{\partial q_{bx}}{\partial \frac{\partial \eta}{\partial y}} + \frac{\partial q_{bky}}{\partial \frac{\partial \eta}{\partial x}} - f_k^I \frac{\partial q_{by}}{\partial \frac{\partial \eta}{\partial x}}\right] & [\mathbb{0}] \end{array}\right] \tag{51}$$

The system matrix in x direction is:

$$\mathbf{A}_x = \left[\begin{array}{ccccc:c} 0 & 1 & 0 & 0 & 0 & [\mathbb{0}] \\ gh - \left(\frac{q_x}{h}\right)^2 & 2\frac{q_x}{h} - \frac{\partial T'_{xx}}{\partial q_x} & -\frac{\partial T'_{xx}}{\partial q_y} & -\frac{\partial T'_{xx}}{\partial I} & gh & [\mathbb{0}] \\ \frac{-q_x q_y}{h^2} & \frac{q_y}{h} - \frac{\partial T'_{yx}}{\partial q_x} & \frac{q_x}{h} - \frac{\partial T'_{yx}}{\partial q_y} & -\frac{\partial T'_{yx}}{\partial I} & 0 & [\mathbb{0}] \\ 0 & -S_{sxx} & -S_{syx} & \frac{q_x}{h} & 0 & [\mathbb{0}] \\ \frac{\partial q_{bx}}{\partial h} & \frac{\partial q_{bx}}{\partial q_x} & \frac{\partial q_{bx}}{\partial q_y} & \frac{\partial q_{bx}}{\partial I} & 0 & \left[\frac{\partial q_{bx}}{\partial M_{al}}\right] \\ \hdashline \left[\frac{\partial q_{bkx}}{\partial h} - f_k^I \frac{\partial q_{bx}}{\partial h}\right] & \left[\frac{\partial q_{bkx}}{\partial q_x} - f_k^I \frac{\partial q_{bx}}{\partial q_x}\right] & \left[\frac{\partial q_{bkx}}{\partial q_y} - f_k^I \frac{\partial q_{bx}}{\partial q_y}\right] & \left[\frac{\partial q_{bkx}}{\partial I} - f_k^I \frac{\partial q_{bx}}{\partial I}\right] & [\mathbb{0}] & \left[\frac{\partial q_{bkx}}{\partial M_{al}} - f_k^I \frac{\partial q_{bx}}{\partial M_{al}}\right] \end{array}\right] \tag{52}$$

The system matrix in y direction is:

$$\mathbf{A}_y = \left[\begin{array}{ccccc:c} 0 & 0 & 1 & 0 & 0 & [0] \\ \frac{-q_x q_y}{h^2} & \frac{q_y}{h} - \frac{\partial T'_{xy}}{\partial q_x} & \frac{q_x}{h} - \frac{\partial T'_{xy}}{\partial q_y} & -\frac{\partial T'_{xy}}{\partial I} & 0 & [\mathbb{0}] \\ gh - \left(\frac{q_y}{h}\right)^2 & -\frac{\partial T'_{yy}}{\partial q_x} & 2\frac{q_y}{h} - \frac{\partial T'_{yy}}{\partial q_y} & -\frac{\partial T'_{yy}}{\partial I} & gh & [\mathbb{0}] \\ 0 & -S_{sxy} & -S_{syy} & \frac{q_y}{h} & 0 & [\mathbb{0}] \\ \frac{\partial q_{by}}{\partial h} & \frac{\partial q_{by}}{\partial q_x} & \frac{\partial q_{by}}{\partial q_y} & \frac{\partial q_{by}}{\partial I} & 0 & \left[\frac{\partial q_{by}}{\partial M_{al}}\right] \\ \hdashline \left[\frac{\partial q_{bky}}{\partial h} - f_k^I \frac{\partial q_{by}}{\partial h}\right] & \left[\frac{\partial q_{bky}}{\partial q_x} - f_k^I \frac{\partial q_{by}}{\partial q_x}\right] & \left[\frac{\partial q_{bky}}{\partial q_y} - f_k^I \frac{\partial q_{by}}{\partial q_y}\right] & \left[\frac{\partial q_{bky}}{\partial I} - f_k^I \frac{\partial q_{by}}{\partial I}\right] & [\mathbb{0}] & \left[\frac{\partial q_{bky}}{\partial M_{al}} - f_k^I \frac{\partial q_{by}}{\partial M_{al}}\right] \end{array}\right] \tag{53}$$

The vector of source terms is:

$$\mathbf{S} = \left[\begin{array}{c} 0 \\ ghS_{fx} \\ ghS_{fy} \\ \frac{QI}{h^2 L_I^*} \\ 0 \\ \hdashline [\mathbb{0}] \end{array}\right] \tag{54}$$

4 Perturbation Analysis

In this Section we conduct a perturbation analysis of the model equations (Section 4.1). We test the linear analysis by means of numerical simulations (Section 4.2).

4.1 Linearization

We consider a reference state of dependent variables $\mathbf{Q_0}$ which is a solution of the equations and a small perturbation to the state $\mathbf{Q'}$ so that $\mathbf{Q} = \mathbf{Q_0} + \mathbf{Q'}$. The reference state is that of steady uniform straight flow in an arbitrary direction over a flat sloping bed composed of an arbitrary uniform grain size distribution.

Mathematically, $h_0 = \text{c1}$, $q_{x0} = \text{c2}$, $q_{y0} = \text{c3}$, $I_0 = 0$, $\frac{\partial \eta}{\partial x} = \text{c4}$, $\frac{\partial \eta}{\partial y} = \text{c5}$, $M_{ak0} = \text{c6}\ \forall k \in \{1, N-1\}$, where c$X$ stands for a constant such that:

$$\begin{aligned}\frac{\partial \mathbf{Q_0}}{\partial t} + \mathbf{D_x}\left(\mathbf{Q_0}\right)\frac{\partial^2 \mathbf{Q_0}}{\partial x^2} + \mathbf{D_y}\left(\mathbf{Q_0}\right)\frac{\partial^2 \mathbf{Q_0}}{\partial y^2} + \mathbf{C}\left(\mathbf{Q_0}\right)\frac{\partial^2 \mathbf{Q_0}}{\partial x \partial y} + \mathbf{A_x}\left(\mathbf{Q_0}\right)\frac{\partial \mathbf{Q_0}}{\partial x} + \mathbf{A_y}\left(\mathbf{Q_0}\right)\frac{\partial \mathbf{Q_0}}{\partial y} + \mathbf{S}\left(\mathbf{Q_0}\right) = 0 \implies \\ \mathbf{A_x}\left(\mathbf{Q_0}\right)\frac{\partial \mathbf{Q_0}}{\partial x} + \mathbf{A_y}\left(\mathbf{Q_0}\right)\frac{\partial \mathbf{Q_0}}{\partial y} + \mathbf{S}\left(\mathbf{Q_0}\right) = 0\end{aligned} \tag{55}$$

We substitute the perturbed solution into the system of equations (47):

$$\begin{aligned}\frac{\partial \mathbf{Q}}{\partial t} + \mathbf{D_x}\left(\mathbf{Q}\right)\frac{\partial^2 \mathbf{Q}}{\partial x^2} + \mathbf{D_y}\left(\mathbf{Q}\right)\frac{\partial^2 \mathbf{Q}}{\partial y^2} + \mathbf{C}\left(\mathbf{Q}\right)\frac{\partial^2 \mathbf{Q}}{\partial x \partial y} + \mathbf{A_x}\left(\mathbf{Q}\right)\frac{\partial \mathbf{Q}}{\partial x} + \mathbf{A_y}\left(\mathbf{Q}\right)\frac{\partial \mathbf{Q}}{\partial y} + \mathbf{S}\left(\mathbf{Q}\right) = 0 \implies \\ \frac{\partial\left(\mathbf{Q_0} + \mathbf{Q'}\right)}{\partial t} + \mathbf{D_x}\left(\mathbf{Q_0} + \mathbf{Q'}\right)\frac{\partial^2\left(\mathbf{Q_0} + \mathbf{Q'}\right)}{\partial x^2} + \mathbf{D_y}\left(\mathbf{Q_0} + \mathbf{Q'}\right)\frac{\partial^2\left(\mathbf{Q_0} + \mathbf{Q'}\right)}{\partial y^2} + \mathbf{C}\left(\mathbf{Q_0} + \mathbf{Q'}\right)\frac{\partial^2\left(\mathbf{Q_0} + \mathbf{Q'}\right)}{\partial x \partial y} + \\ + \mathbf{A_x}\left(\mathbf{Q_0} + \mathbf{Q'}\right)\frac{\partial\left(\mathbf{Q_0} + \mathbf{Q'}\right)}{\partial x} + \mathbf{A_y}\left(\mathbf{Q_0} + \mathbf{Q'}\right)\frac{\partial\left(\mathbf{Q_0} + \mathbf{Q'}\right)}{\partial y} + \mathbf{S}\left(\mathbf{Q_0} + \mathbf{Q'}\right) = 0\end{aligned} \tag{56}$$

The terms of the matrices $\mathbf{D_x}$, $\mathbf{D_y}$, $\mathbf{C}$, $\mathbf{A_x}$, and $\mathbf{A_y}$ evaluated at $(\mathbf{Q_0} + \mathbf{Q'})$ are linearized such that:

$$\mathbf{G}\left(\mathbf{Q_0} + \mathbf{Q'}\right) = \mathbf{G}\left(\mathbf{Q_0}\right) + \mathbf{G_J}\left(\mathbf{Q_0}\right)\mathbf{Q'} + \mathcal{O}\left(\mathbf{Q'}^2\right) \tag{57}$$

where $\mathbf{G}$ is one of the matrices and $\mathbf{G_J}$ is a matrix that contains the first order terms. For instance, for the first term of the momentum equation in the x direction we obtain:

$$\begin{aligned}gh - \left(\frac{q_x}{h}\right)^2 = g\left(h_0 + h'\right) - \left(\frac{\left(q_{x0} + q'_x\right)}{\left(h_0 + h'\right)}\right)^2 = \\ = gh_0 + gh' - \left(q_{x0}^2 + q_x^{'2} + 2q_{x0}q'_x\right)\left(h_0^{-2} - 2h_0^3 h'\right) = \\ = gh_0 - \left(\frac{q_{x0}}{h_0}\right)^2 + \left(g + \frac{q_{x0}^2}{h_0^3}\right)h' + 2\frac{q_{x0}}{h_0^2}q'_x - h_0^{-2}q_x^{'2} + 2h_0^{-3}h'q_x^{'2} - 4h_0^{-3}q_{x0}q'_x h'\end{aligned} \tag{58}$$

Neglecting secondary terms we obtain:

$$\mathbf{D_j}\left(\mathbf{Q_0} + \mathbf{Q'}\right)\frac{\partial^2\left(\mathbf{Q_0} + \mathbf{Q'}\right)}{\partial j^2} = \left[\mathbf{D_j}\left(\mathbf{Q_0}\right) + \mathbf{D_{Jj}}\left(\mathbf{Q_0}\right)\mathbf{Q'}\right]\left[\frac{\partial^2 \mathbf{Q_0}}{\partial j^2} + \frac{\partial^2 \mathbf{Q'}}{\partial j^2}\right] = \mathbf{D_j}\left(\mathbf{Q_0}\right)\frac{\partial^2 \mathbf{Q'}}{\partial j^2} \tag{59}$$

$$\mathbf{C}\left(\mathbf{Q_0} + \mathbf{Q'}\right)\frac{\partial^2\left(\mathbf{Q_0} + \mathbf{Q'}\right)}{\partial x y} = \left[\mathbf{C}\left(\mathbf{Q_0}\right) + \mathbf{C_J}\left(\mathbf{Q_0}\right)\mathbf{Q'}\right]\left[\frac{\partial^2 \mathbf{Q_0}}{\partial x y} + \frac{\partial^2 \mathbf{Q'}}{\partial x y}\right] = \mathbf{C}\left(\mathbf{Q_0}\right)\frac{\partial^2 \mathbf{Q'}}{\partial x y} \tag{60}$$

$$\mathbf{A_j}\left(\mathbf{Q_0} + \mathbf{Q'}\right)\frac{\partial\left(\mathbf{Q_0} + \mathbf{Q'}\right)}{\partial j} = \left[\mathbf{A_j}\left(\mathbf{Q_0}\right) + \mathbf{A_{Jj}}\left(\mathbf{Q_0}\right)\mathbf{Q'}\right]\left[\frac{\partial \mathbf{Q_0}}{\partial j} + \frac{\partial \mathbf{Q'}}{\partial j}\right] = \mathbf{A_{Jj}}\left(\mathbf{Q_0}\right)\mathbf{Q'}\frac{\partial \mathbf{Q_0}}{\partial j} + \mathbf{A_j}\left(\mathbf{Q_0}\right)\frac{\partial \mathbf{Q'}}{\partial j} \tag{61}$$

where subindex $j = x, y$. We have used that $\frac{\partial^2 \mathbf{Q_0}}{\partial j^2} = 0$ and that $\mathbf{G_J}\left(\mathbf{Q_0}\right)\mathbf{Q'}\frac{\partial^2 \mathbf{Q'}}{\partial j^2}$ is negligible. Note that $\frac{\partial \mathbf{Q_0}}{\partial j} \neq 0$ because the bed slope is not zero. In this case:

$$gh\frac{\partial \eta}{\partial j} = g\left(h_0 + h'\right)\frac{\partial\left(\eta_0 + \eta'\right)}{\partial j} = gh_0\frac{\partial \eta_0}{\partial j} + gh_0\frac{\partial \eta'}{\partial j} + gh'\frac{\partial \eta_0}{\partial j} \tag{62}$$

where we have neglected secondary terms. The first right hand side term is part of $\mathbf{A_j}\left(\mathbf{Q_0}\right)\frac{\partial \mathbf{Q_0}}{\partial j}$, the second term is part of $\mathbf{A_j}\left(\mathbf{Q_0}\right)\frac{\partial \mathbf{Q'}}{\partial j}$ and the third term is the only term of $\mathbf{A_{Jj}}\left(\mathbf{Q_0}\right)\mathbf{Q'}\frac{\partial \mathbf{Q_0}}{\partial j}$. Thus, we write:

$$\mathbf{A_{Jt}} = \left(\mathbf{A_{Jx}}\left(\mathbf{Q_0}\right)\frac{\partial \mathbf{Q_0}}{\partial x} + \mathbf{A_{Jy}}\left(\mathbf{Q_0}\right)\frac{\partial \mathbf{Q_0}}{\partial y}\right)\mathbf{Q'} = \left[\begin{array}{ccccc:c} 0 & 0 & 0 & 0 & 0 & [\mathbb{0}] \\ g\frac{\partial \eta_0}{\partial x} & 0 & 0 & 0 & 0 & [\mathbb{0}] \\ g\frac{\partial \eta_0}{\partial y} & 0 & 0 & 0 & 0 & [\mathbb{0}] \\ 0 & 0 & 0 & 0 & 0 & [\mathbb{0}] \\ 0 & 0 & 0 & 0 & 0 & [\mathbb{0}] \\ \hdashline [\mathbb{0}] & [\mathbb{0}] & [\mathbb{0}] & [\mathbb{0}] & [\mathbb{0}] & [\mathbb{0}] \end{array}\right] \tag{63}$$

where $\frac{\partial \eta_0}{\partial j} = -\frac{C_f q_{j0} Q_0}{g h_0^3}$ which we obtain from the fact that $\mathbf{Q_0}$ is a uniform steady solution.

The source term is linearized:

$$\mathbf{S}\left(\mathbf{Q_0} + \mathbf{Q'}\right) = \mathbf{S}\left(\mathbf{Q_0}\right) + \mathbf{S_J}\left(\mathbf{Q_0}\right)\mathbf{Q'} + \mathcal{O}\left(\mathbf{Q'}^2\right) \tag{64}$$

where $\mathbf{S_J}$ is the jacobian of S:

$$\mathbf{S_J} = \left[\begin{array}{ccccc:c} 0 & 0 & 0 & 0 & 0 & [\mathbb{0}] \\ \frac{-2QC_f q_x}{h^3} & \frac{C_f\left(Q^2+q_x^2\right)}{h^2 Q} & \frac{C_f q_x q_y}{Q h^2} & 0 & 0 & [\mathbb{0}] \\ \frac{-2QC_f q_y}{h^3} & \frac{C_f q_x q_y}{Q h^2} & \frac{C_f\left(Q^2+q_y^2\right)}{h^2 Q} & 0 & 0 & [\mathbb{0}] \\ \frac{-2QI}{L_I^* h^3} & \frac{q_x I}{L_I^* h^2 Q} & \frac{q_y I}{L_I^* h^2 Q} & \frac{Q}{L_I^* h^2} & 0 & [\mathbb{0}] \\ 0 & 0 & 0 & 0 & 0 & [\mathbb{0}] \\ \hdashline [\mathbb{0}] & [\mathbb{0}] & [\mathbb{0}] & [\mathbb{0}] & [\mathbb{0}] & [\mathbb{0}] \end{array}\right] \tag{65}$$

Substituting Equations (59), (60), (61), (63), and (64) in Equation (56) and using the fact $\mathbf{Q_0}$ satisfies Equation (47 we obtain:

$$\frac{\partial \mathbf{Q'}}{\partial t} + \mathbf{D_{x0}}\frac{\partial^2 \mathbf{Q'}}{\partial x^2} + \mathbf{D_{y0}}\frac{\partial^2 \mathbf{Q'}}{\partial y^2} + \mathbf{C_0}\frac{\partial^2 \mathbf{Q'}}{\partial x \partial y} + \mathbf{A_{x0}}\frac{\partial \mathbf{Q'}}{\partial x} + \mathbf{A_{y0}}\frac{\partial \mathbf{Q'}}{\partial y} + \mathbf{B_0}\mathbf{Q'} = 0 \tag{66}$$

where the subindex $_\mathbf{0}$ indicates that the matrix is evaluated at the unperturbed state and $\mathbf{B} = \mathbf{S_J} + \mathbf{A_{Jt}}$.

Assuming a wave type perturbation $\mathbf{Q'} = \hat{\mathbf{Q}}\left(t\right)e^{ik_x x + ik_y y}$ where i is the imaginary unit and k_x and k_y are wave numbers in x and y direction respectively and $\hat{\mathbf{Q}}\left(t\right)$ is a time dependent amplitude we obtain the system:

$$\begin{aligned} \frac{\partial \hat{\mathbf{Q}}\left(t\right)}{\partial t} - \mathbf{D_{x0}}k_x^2\hat{\mathbf{Q}}\left(t\right) - \mathbf{D_{y0}}k_y^2\hat{\mathbf{Q}}\left(t\right) - \mathbf{C_0}k_x k_y\hat{\mathbf{Q}}\left(t\right) + \mathbf{A_{x0}}ik_x\hat{\mathbf{Q}}\left(t\right) + \mathbf{A_{y0}}ik_y\hat{\mathbf{Q}}\left(t\right) + \mathbf{B_0}\hat{\mathbf{Q}}\left(t\right) = 0 \implies \\ \frac{\partial \hat{\mathbf{Q}}\left(t\right)}{\partial t} = \left[\mathbf{D_{x0}}k_x^2 + \mathbf{D_{y0}}k_y^2 + \mathbf{C_0}k_x k_y - \mathbf{A_{x0}}ik_x - \mathbf{A_{y0}}ik_y - \mathbf{B_0}\right]\hat{\mathbf{Q}}\left(t\right) \ . \end{aligned} \tag{67}$$

Using the properties of the eigenvalues we obtain the ordinary differential equation:

$$\frac{\mathrm{d}\mathbf{\Phi}}{\mathrm{d}t} = \lambda\mathbf{\Phi} \ , \tag{68}$$

where $\mathbf{\Phi}$ and λ are an eigenvector and eigenvalue of matrix

$$\mathbf{R} = \mathbf{D_{x0}}k_x^2 + \mathbf{D_{y0}}k_y^2 + \mathbf{C_0}k_x k_y - \mathbf{A_{x0}}ik_x - \mathbf{A_{y0}}ik_y - \mathbf{B_0} \ , \tag{69}$$

respectively. The real part of $\lambda_m \ \forall m \in \{1, N+4\}$ is the growth rate of the perturb solution. The imaginary part yields the propagation speed.

4.2 Test Using Numerical Simulations

In this Section we test the linear stability analysis. To this end we study the initial development of free alternate bars in straight channels which are recognized to be the result of an instability mechanism (*Engelund and Skovgaard*, 1973; *Parker*, 1976; *Fredsœ*, 1978; *Olesen*, 1982, 1983; *Kuroki and Kishi*, 1984; *Ikeda*, 1984; *Jaeggi*, 1984; *Colombini et al.*, 1987; *Tubino*, 1991; *Schielen et al.*, 1993; *Tubino et al.*, 1999; *Lanzoni*, 2000). We compare the linear theory with the results of numerical simulations using Delft3D following a similar strategy as *Siviglia et al.* (2013).

The linear analysis predicts the stability or instability of a combinations of wave numbers in streamwise and transverse direction for a given a reference state. That is, a double-periodic perturbation (characterized by a

certain wave number in x and y direction) is added to a uniform flow and if the real part of all the eigenvalues of the resulting system, Equation (69), are negative, the perturbations will decay. If at least one is positive, they will grow.

We consider a uniform state with the parameters shown in Table 2. We consider unisize sediment. The sediment transport rate is computed using the relation by *Engelund and Hansen* (1967). The bed slope effects are taken into account using the relation by *Sekine and Parker* (1992). This is equivalent to use the relation by *Koch and Flokstra* (1980), Equation (18), with parameters $A_s = 1$, $B_s = 0$, $C_s = 0$, and $D_s = 0$. The instability domain of the reference state is plotted in Figure 1. The curves are the separatrix between the linearly stable and unstable domains (i.e., growth rate, real part of the eigenvalues, equal to 0). The continuous line is obtained assuming no secondary flow while the discontinuous line considers secondary flow with a diffusion coefficient $D_H = 5\,\mathrm{m}^2/\mathrm{s}$. The left plot presents the domain in terms of wave number. The right plot present the same domain in terms of wavelength. Due to the impermeable boundary conditions at the closed domains (i.e., the river banks), only natural multiples of π are valid transverse wave numbers. Since the first mode (i.e., transverse bars) is the most unstable one (*Colombini et al.*, 1987; *Schielen et al.*, 1993), the width is obtained as π/k_{wy}. Note that secondary flow reduces the unstable domain thus reducing the conditions in which bars grow.

u [m/s]	v [m/s]	h [m]	C_f [−]	d_k [m]	s [−]	q_{bk} [m^2/s]
1	0	1	0.007	0.001	$7.135\,41 \times 10^{-4}$	1.118×10^{-4}

Table 2: Physical parameters of the reference state to test linear analysis.

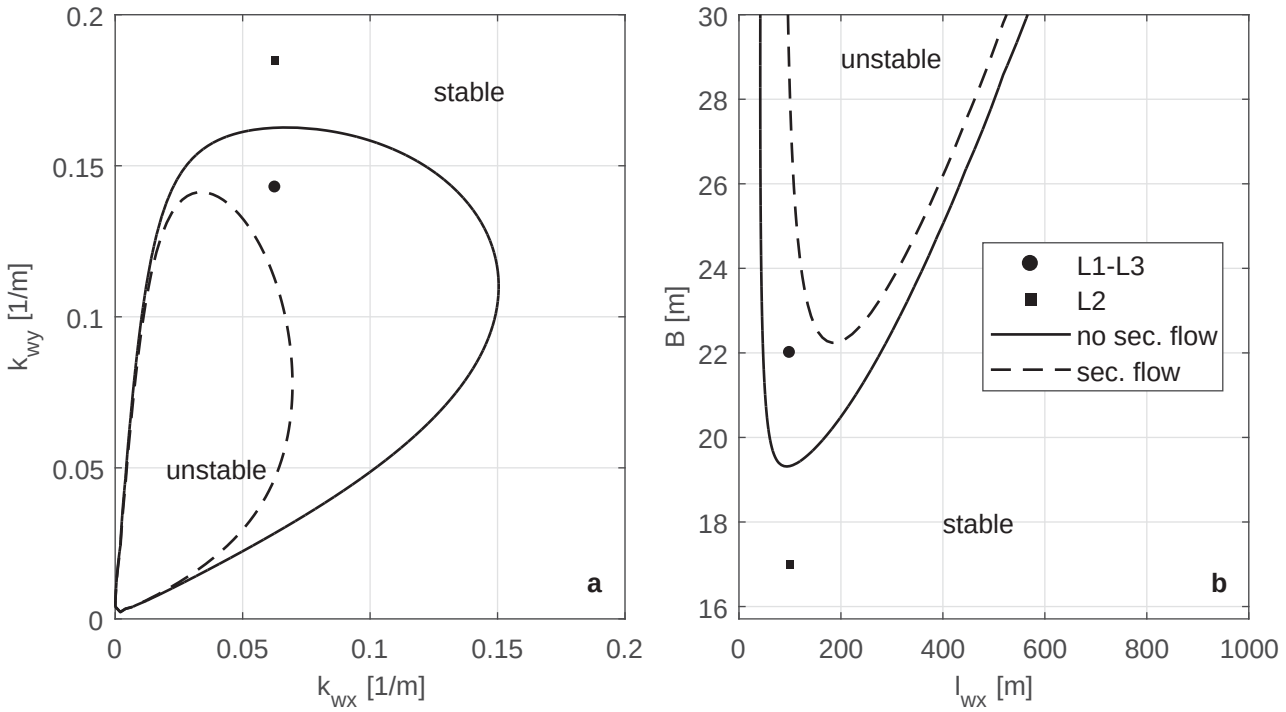

Figure 1: Domain of linear stability of the reference situation (Table 2) in terms of: (**a**) wavenumber, and (**b**) wave length. The continuous line is the separatrix for the case without secondar flow while the dashed line is the separatrix considering secondary flow and a diffusion coefficient $D_H = 5\,\mathrm{m}^2/\mathrm{s}$. The circle and square mark the conditions of the numerical simulations (Table 4).

We conduct three numerical simulations varying the width and the consideration of secondary flow (Figure 1). The simulations start under the equilibrium conditions of the uniform reference state in which a double-periodic perturbation in bed elevation that satisfies the boundary conditions is added:

$$\eta' = A \sin\left(\frac{\pi y}{B}\right) \cos\left(\frac{2\pi x}{L_b} - \frac{\pi}{2}\right) , \tag{70}$$

where $A = 0.005\,\mathrm{m}$ is the amplitude, B [m] is the width, and $L_b = 100\,\mathrm{m}$ is the streamwise wavelength. The channel is aligned with the x axis with the origin at the center of the channel. Table 3 presents the parameters

which are equal for all simulations and Table 4 presents the ones which are different. The simulations have a spin up time of 1800 s for the flow to adapt to the perturbed initial condition. We have visually checked that after the spin up time the flow is steady.

L [m]	Δt [s]	Δx [m]	Δy [m]	T [s]
1000	1	1	1	$(1800) + 3600$

Table 3: Parameters which are equal for the simulations to test the linear analysis. The symbols not defined previously are the length of the domain L [m], the time step Δt [s], the space step in the x direction Δx [m], the space step in y direction [m], and the simulation time T [s]. The time in parenthesis is the spin-up time.

Simulation	B [m]	sec. flow	linear analysis
L1	22	N	growth
L2	17	N	decay
L3	22	Y	decay

Table 4: Parameters which are different for the simulations to test the linear analysis.

In Figure 2 we show the evolution of the flow depth with time at $y = B/2$ for a location in which initially we find the trough of a bar (i.e., maximum flow depth). For the three numerical simulations the initial perturbation grows or decays as predicted in the linear analysis.

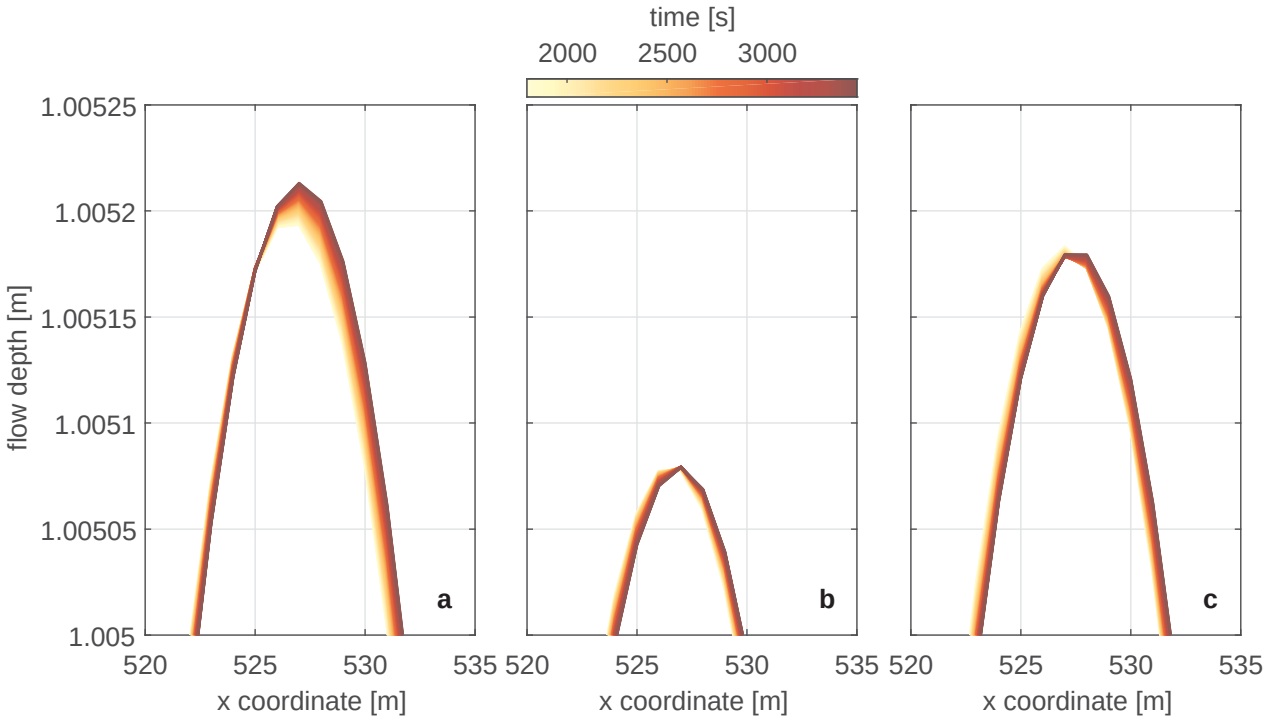

Figure 2: Domain of linear stability of the reference situation (Table 2) in terms of: (**a**) wavenumber, and (**b**) wave length. The continuous line is the separatrix for the case without secondar flow while the dashed line is the separatrix considering secondary flow and a diffusion coefficient $D_H = 5\,\mathrm{m}^2/\mathrm{s}$. The circle and square mark the conditions of the numerical simulations (Table 4).

5 Results of the Linear Analysis

In this section we apply the results of the linear analysis to study the effects of secondary flow and bed slope effects on the mathematical character of the system of equations.

5.1 Definition of Ill-posedness

In this section we describe the conditions

- Hadamard definition
- dampening of oscillations for increasing kwx and kwy
- the largest degree rules
- friction does not affect
- if no diffusion in all equations
- if diffusion in not all equations
- if no diffusion only eigenvalues of Ax i Ay
- possible role of eigenvectors

5.2 Secondary Flow in a Unisize Sediment Case

- ill-posed if sec flow but no diffusion 020
- role of diffusion

5.3 Secondary Flow in a Mixed-size Sediment Case

5.4 Bed Slope Effect in a Unisize Sediment Case

5.5 Bed Slope Effect in a Mixed-size Sediment Case

6 Ill-posedness Check in Delft3D

In this section we test the implementation of the ellipticity check in Delft3D.

6.1 Implementation Test Without Considering Secondary Flow nor Bed Slope Effects

In this section we test the implementation of the ellipticity check under conditions without secondary flow nor including the effects of bed slope on the sediment transport. Under these conditions the system of equations (47) does not have diffusive terms. Moreover, the well-posedness of the system is not influenced by the source terms (Section 4.2). Thus, the test is based solely on the analysis of the matrices in Equations (52) and (53). *Chavarrías and Ottevanger* (2016) checked that the matrices were correctly implemented. Here we test that the eigenvalues are correctly computed and that the output is correctly passed.

We use the same three test simulations as in *Chavarrías and Ottevanger* (2016). The simulations are 2 dimensional. The domain is rectangular with two open boundaries on opposite ends. The initial condition is in equilibrium for a certain upstream water and sediment discharge and a certain downstream water level. The initial water and sediment discharge remain constant throughout the simulation time. A slow lowering (0.001 m/min) of the downstream water level is imposed that causes degradational conditions. The simulations differ in the number of size fractions and the initial stratigraphy. Table 5 summarizes the initial conditions and physical parameters that are the same for all simulations. Table 6 contains the initial conditions and physical parameters which are different between simulations. Table 7 summarizes the numerical parameters of the simulations.

L [m]	B [m]	u [m/s]	v [m/s]	h [m]	C_f [−]	L_a [m]	s [−]
1	1	1	0	1	0.007	0.1	$7.13541 \cdot 10^{-4}$

Table 5: Physical parameters of the simulations to test the implementation that are equal for all simulations

Simulation	d_k [m]	F_{ak} [−]	f_k^I [−]	q_{bk} [m^2/s]	Sed. Trans.	Math. Charac.
I1	[0.001, 0.002]	[0.50, 0.50]	[0.50, 0.50]	$[5.588, 2.794] \cdot 10^{-5}$	EH	W
I2	[0.001, 0.002]	[1.00, 0.00]	[0.00, 0.00]	$[0.000, 5.588] \cdot 10^{-5}$	EH	I
I3	[0.001, 0.002, 0.004]	[0.33, 0.33, 0.33]	[0.33, 0.33, 0.33]	$[6.723, 6.319, 5.865] \cdot 10^{-5}$	MPM-P0.8	W

Table 6: Physical parameters of the simulations to test the implementation that are different for all simulations. EH stands for *Engelund and Hansen* (1967) and MPM-P0.8 stands for *Meyer-Peter and Müller* (1948) with the hiding correction by *Parker et al.* (1982) with parameter b=0.8. W means well-posed and I ill-posed.

Δt [s]	Δx [m]	Δy [m]	Δz [m]	T [s]
0.1	0.5	0.5	0.5	60

Table 7: Numerical parameters of the simulations to test the implementation

The symbols not defined previously are the length L [m] and width B [m] of the domain, the bed slope s [−], the time step Δt [s], the space step in the x direction Δx [m], the space step in y direction [m], the thickness of the substrate layers Δz [m], and the simulation time T [s].

In Tables 8 and 9 we show the eigenvalues of matrices $\mathbf{A_x}$ and $\mathbf{A_y}$, respectively, as computed for the reference situation using Matlab. In Tables 10 and 11 we show the eigenvalues given in Delft3D at the node $n = 2$ and $m = 2$ at $t = 2$ s. The minimal difference is mainly due to the fact that while the eigenvalues computed in matlab are those at the exact reference situation, the ones in Delft3D are computed with the flow conditions after 2 s.

Eigenvalue	**I**	I2	I3
λ_1	$+4.133 + 0.000\text{i}$	$+4.133 + 0.000\text{i}$	$+4.134 + 0.000\text{i}$
λ_2	$-2.134 + 0.000\text{i}$	$-2.133 + 0.000\text{i}$	$-2.135 + 0.000\text{i}$
λ_3	$(+6.216 + 0.000\text{i}) \times 10^{-4}$	$(+7.251 + 6.630\text{i}) \times 10^{-4}$	$(+1.382 + 0.000\text{i}) \times 10^{-3}$
λ_4	$(+1.552 + 0.000\text{i}) \times 10^{-3}$	$(+7.251 - 6.630\text{i}) \times 10^{-4}$	$(+3.258 + 0.000\text{i}) \times 10^{-3}$
λ_5	$+1.000 + 0.000\text{i}$	$+1.000 + 0.000\text{i}$	$(+2.995 + 0.000\text{i}) \times 10^{-3}$
λ_6		$+0.000 + 0.000\text{i}$	$+1.000 + 0.000\text{i}$

Table 8: Eigenvalues in the x direction for the reference situation computed with Matlab.

Eigenvalue	**I**	I2	I3
λ_1	$+3.132 + 0.000\text{i}$	$+3.132 + 0.000\text{i}$	$-3.133 + 0.000\text{i}$
λ_2	$-3.132 + 0.000\text{i}$	$-3.132 + 0.000\text{i}$	$+3.133 + 0.000\text{i}$
λ_3	$+0.000 + 0.000\text{i}$	$+0.000 + 0.000\text{i}$	$+0.000 + 0.000\text{i}$
λ_4	$+0.000 + 0.000\text{i}$	$+0.000 + 0.000\text{i}$	$+0.000 + 0.000\text{i}$
λ_5	$+0.000 + 0.000\text{i}$	$+0.000 + 0.000\text{i}$	$+0.000 + 0.000\text{i}$
λ_6	$+0.000 + 0.000\text{i}$	$+0.000 + 0.000\text{i}$	$+0.000 + 0.000\text{i}$

Table 9: Eigenvalues in the y direction for the reference situation computed with Matlab.

Eigenvalue	**I**	I2	I3
λ_1	$+4.133 + 0.000\text{i}$	$+4.133 + 0.000\text{i}$	$+4.133 + 0.000\text{i}$
λ_2	$-2.134 + 0.000\text{i}$	$-2.133 + 0.000\text{i}$	$-2.135 + 0.000\text{i}$
λ_3	$(+6.216 + 0.000\text{i}) \times 10^{-4}$	$(+7.249 + 6.622\text{i}) \times 10^{-4}$	$(+1.383 + 0.000\text{i}) \times 10^{-3}$
λ_4	$(+1.552 + 0.000\text{i}) \times 10^{-3}$	$(+7.249 - 6.622\text{i}) \times 10^{-4}$	$(+3.261 + 0.000\text{i}) \times 10^{-3}$
λ_5	$+1.000 + 0.000\text{i}$	$+1.000 + 0.000\text{i}$	$(+2.998 + 0.000\text{i}) \times 10^{-3}$
λ_6		$+0.000 + 0.000\text{i}$	$+1.000 + 0.000\text{i}$

Table 10: Eigenvalues in the x direction computed in Delft3D.

- check output elliptic/hyperbolic

Eigenvalue	**I**	I2	I3
λ_1	$+3.132 + 0.000\mathrm{i}$	$+3.132 + 0.000\mathrm{i}$	$-3.132 + 0.000\mathrm{i}$
λ_2	$-3.132 + 0.000\mathrm{i}$	$-3.132 + 0.000\mathrm{i}$	$+3.132 + 0.000\mathrm{i}$
λ_3	$+0.000 + 0.000\mathrm{i}$	$+0.000 + 0.000\mathrm{i}$	$+0.000 + 0.000\mathrm{i}$
λ_4	$+0.000 + 0.000\mathrm{i}$	$+0.000 + 0.000\mathrm{i}$	$+0.000 + 0.000\mathrm{i}$
λ_5	$+0.000 + 0.000\mathrm{i}$	$+0.000 + 0.000\mathrm{i}$	$+0.000 + 0.000\mathrm{i}$
λ_6	$+0.000 + 0.000\mathrm{i}$	$+0.000 + 0.000\mathrm{i}$	$+0.000 + 0.000\mathrm{i}$

Table 11: Eigenvalues in the y direction computed in Delft3D.

6.2 Implementation Test Considering Secondary Flow and Bed Slope Effects

6.3 Experiment by *Ashida et al.* (1990)

6.4 DVR Simulation

7 Discussion

- Perturb around a state with secondary flow intensity equal to equlibrium. That is, perturb around equilibrium solution of flow in a bend rather than flat bed no circular flow.
- possible role of eigenvectors

8 Conclusions

- role of diffusion in secondary flow formulation
- implementation validated in Delft3D

References

Blom, A. (2008), Different approaches to handling vertical and streamwise sorting in modeling river morphodynamics, *Water Resour. Res.*, *44*(3), W03,415, doi:10.1029/2006WR005474.

Blom, A., J. S. Ribberink, and H. J. de Vriend (2003), Vertical sorting in bed forms: Flume experiments with a natural and a trimodal sediment mixture, *Water Resour. Res.*, *39*(2), 1025, doi:10.1029/2001WR001088.

Blom, A., G. Parker, J. S. Ribberink, and H. J. de Vriend (2006), Vertical sorting and the morphodynamics of bed-form-dominated rivers: An equilibrium sorting model, *J. Geophys. Res., Earth Surface*, *111*, F01,006, doi:10.1029/2004JF000175.

Blom, A., J. S. Ribberink, and G. Parker (2008), Vertical sorting and the morphodynamics of bed form-dominated rivers: A sorting evolution model, *J. Geophys. Res., Earth Surface*, *113*, F01,019, doi:10.1029/2006JF000618.

Blom, A., E. Viparelli, and V. Chavarrías (2016), The graded alluvial river: Profile concavity and downstream fining, *Geophys. Res. Lett.*, *43*, 1–9, doi:10.1002/2016GL068898.

Chavarrías, V., and W. Ottevanger (2016), Mathematical analysis of the well-posedness of the Hirano active layer concept in 2D models, *Tech. Rep. 1230044*, Deltares.

Chavarrías, V., G. Stecca, R. J. Labeur, and A. Blom (), Ill-posedness in modelling mixed-sediment river morphodynamics, (submitted to Advances in Water Resources).

Colombini, M., G. Seminara, and M. Tubino (1987), Finite-amplitude alternate bars, *J. Fluid Mech.*, *181*, 213–232, doi:10.1017/S0022112087002064.

Egiazaroff, I. V. (1965), Calculation of nonuniform sediment concentrations, *J. Hydraulics Div.*, *91*(4), 225–247.

Engelund, F., and E. Hansen (1967), Monograph on sediment transport in alluvial streams, *Tech. Rep.*, Hydraul. Lab., Tech. Univ. of Denmark, Copenhagen, Denmark., 63 pp.

Engelund, F., and O. Skovgaard (1973), On the origin of meandering and braiding in alluvial streams, *J. Fluid Mech.*, *57*(2), 289–302, doi:10.1017/S0022112073001163.

Fredsœ, J. (1978), Meandering and braiding of rivers, *J. Fluid Mech.*, *84*(4), 609–624, doi:10.1017/S0022112078000373.

Hirano, M. (1971), River bed degradation with armoring, *Trans. Jpn. Soc. Civ. Eng*, *195*, 55–65, doi:10.2208/jscej1969.1971.195_55.

Hoey, T. B., and R. Ferguson (1994), Numerical simulation of downstream fining by selective transport in gravel bed rivers: Model development and illustration, *Water Resour. Res.*, *30*(7), 2251–2260, doi:10.1029/94WR00556.

Ikeda, S. (1984), Prediction of alternate bar wavelength and height, *Journal of Hydraulic Engineering*, *110*(4), doi:10.1061/(ASCE)0733-9429(1984)110:4(371).

Jaeggi, M. N. R. (1984), Formation and effects of alternate bars, *J. Hydraul. Eng.*, *110*(2), 142–156, doi:10.1061/(ASCE)0733-9429(1984)110:2(142).

Joseph, D., and J. Saut (1990), Short-wave instabilities and ill-posed initial-value problems, *Theor. Comput. Fluid Mech.*, *1*(4), 191–227, doi:10.1007/BF00418002.

Kalkwijk, J. P. T., and R. Booij (1986), Adaptation of secondary flow in nearly-horizontal flow, *J. Hydraul. Res.*, *24*(1), 19–37, doi:10.1080/00221686609499330.

Koch, F. G., and C. Flokstra (1980), Bed level computations for curved alluvial channels, *Tech. Rep. 240*, Delft Hydraulics Laboratory, The Netherlands.

Kuroki, M., and T. Kishi (1984), Regime criteria on bars and braids in alluvial straight channels, *Proceedings of the Japanese Society of Civil Engineers*, *342*, 87–96, (in Japanese).

Lanzoni, S. (2000), Experiments on bar formation in a straight flume: 1. Uniform sediment, *Water Resour. Res.*, *36*(11), 3337–3349, doi:10.1029/2000WR900160.

Lanzoni, S., and M. Tubino (1999), Grain sorting and bar instability, *J. Fluid Mech.*, *393*, 149–174, doi:10.1017/S0022112099005583.

Meyer-Peter, E., and R. Müller (1948), Formulas for bed-load transport, in *Proc. 2nd Meeting Int. Assoc. Hydraul. Struct. Res.*, pp. 39–64, Stockholm.

Olesen, K. W. (1982), Influence of secondary flow on meandering rivers, *Tech. Rep. 1-82*, Laboratory of Fluid Mechanics, Delft University of Technology.

Olesen, K. W. (1983), Alternate bars in and meandering of alluvial rivers, *Tech. Rep. 83-1*, WL Delft Hydraulics.

Parker, G. (1976), On the cause and characteristic scales of meandering and braiding in rivers, *J. Fluid Mech.*, *76*(3), 457–480, doi:10.1017/S0022112076000748.

Parker, G. (1991), Selective sorting and abrasion of river gravel. I: Theory, *J. Hydraul. Eng.*, *117*(2), 131–147, doi:10.1061/(ASCE)0733-9429(1991)117:2(131).

Parker, G., and P. C. Klingeman (1982), On why gravel bed streams are paved, *Water Resour. Res.*, *18*(5), 1409–1423, doi:10.1029/WR018i005p01409.

Parker, G., P. C. Klingeman, and D. G. McLean (1982), Bedload and size distribution in paved gravel-bed streams, *J. Hydraulics Div.*, *108*(4), 544–571.

Ribberink, J. S. (1987), Mathematical modelling of one-dimensional morphological changes in rivers with non-uniform sediment, Ph.D. thesis, Delft University of Technology, The Netherlands.

Saint-Venant, A. J. C. B. (1871), Théorie du mouvement non permanent des eaux, avec application aux crues des rivières et à l'introduction des marées dans leur lit, *Comptes Rendus des séances de l'Académie des Sciences*, *73*, 237–240, (in French).

Schielen, R., A. Doelman, and H. E. de Swart (1993), On the nonlinear dynamics of free bars in straight channels, *J. Fluid Mech.*, *252*, 325–356, doi:10.1017/S0022112093003787.

Sekine, M., and G. Parker (1992), Bed-load transport on transverse slope. i, *J. Hydraul. Eng.*, *118*(4), 513–535, doi:10.1061/(ASCE)0733-9429(1992)118:4(513).

Seminara, G., M. Colombini, and G. Parker (1996), Nearly pure sorting waves and formation of bedload sheets, *J. Fluid Mech.*, *312*, 253–278, doi:10.1017/S0022112096001991.

Sieben, J. (1997), Modelling of hydraulics and morphology in mountain rivers, Ph.D. thesis, Delft University of Technology.

Siviglia, A., G. Stecca, D. Vanzo, G. Zolezzi, E. F. Toro, and M. Tubino (2013), Numerical modelling of two-dimensional morphodynamics with applications to river bars and bifurcations, *Adv. Water Resour.*, *52*, 243–260, doi:10.1016/j.advwatres.2012.11.010.

Stecca, G., A. Siviglia, and A. Blom (2014), Mathematical analysis of the Saint-Venant-Hirano model for mixed-sediment morphodynamics, *Water Resour. Res.*, *50*, 7563–7589, doi:10.1002/2014WR015251.

Sternberg, H. (1875), Untersuchungen über Längen- und Querprofil geschiebeführender Flüsse, *Zeitschrift für Bauwesen*, *25*, 483–506, (in German).

Talmon, A., N. Struiksma, and M. V. Mierlo (1995), Laboratory measurements of the direction of sediment transport on transverse alluvial-bed slopes, *Journal of Hydraulic Research*, *33*(4), doi:10.1080/00221689509498657.

Thomson, J. (1876), On the origin of windings of rivers in alluvial plains, with remarks on the flow of water round bends in pipes, *Proc. Roy. Soc. London*, *25*(171-178), 5–8, doi:10.1098/rspl.1876.0004.

Tubino, M. (1991), Growth of alternate bars in unsteady flow, *Water Resour. Res.*, *27*(1), 37–52, doi:10.1029/90WR01699.

Tubino, M., R. Repetto, and G. Zolezzi (1999), Free bars in rivers, *J Hydraul Res*, *37*(6), 759–775, doi:10.1080/00221689909498510.

Viparelli, E., R. R. H. Moreira, and A. Blom (2017), *Gravel-Bed Rivers: Process and Disasters*, chap. 23: Modelling stratigraphy-based GBR morphodynamics., pp. 609–637, Wiley-Blackwell, doi:10.1002/9781118971437.ch23.

Yatsu, E. (1955), On the longitudinal profile of the graded river, *EOS, Trans. Am. Geophys. Union*, *36(4)*, 655–663.

Zimmerman, C., and J. F. Kennedy (1978), Transverse bed slopes in curved alluvial streams, *J. Hydraulics Div.*, *104*(1), 33–48.